

THE POLAR CUSP: OPTICAL AND PARTICLE CHARACTERISTICS-DYNAMICS

P. E. SANDHOLT¹, A. EGELAND¹, S. ÅSHEIM¹,
B. LYBEKK¹ and D. A. HARDY²

¹*Institute of Physics, University of Oslo, P.O. Box. 1048, Blindern, 0316 Oslo 3, Norway*

²*Air Force Geophysics Laboratory, Hanscom Air Force Base,
Massachusetts 01731, U.S.A.*

Abstract: Photometric observations from two stations on Svalbard, Norway, have been used to map the location and dynamics of polar cusp auroras. Coordinated observations of low-energy electron precipitation from satellite HILAT and optical observations from the ground are discussed. Cases are presented showing the dynamical behaviour of cusp auroras and the local magnetic field related to changes in the interplanetary magnetic field (IMF) and irregularities in the solar wind plasma. Dynamical phenomena with different time scales are studied. South- and northward expansions of the midday sector of the auroral oval are discussed in relation to IMF variations and geomagnetic substorm activity. Intensifications and rapid poleward motions of discrete auroral structures in the cusp region are shown to be associated with local Pi-type magnetic pulsations, each event lasting a few minutes. These small-scale dynamical phenomena are discussed in relation to different models of plasma penetration across the dayside magnetopause, from the magnetosheath to the polar cusp region of the magnetosphere.

1. Introduction

The dayside aurora is one signature of the polar cusp—a unique localized region in the dayside high latitude magnetosphere with a cusp-like magnetic field configuration due to the interaction with the solar wind. In the polar cusp the solar wind plasma has direct access to the magnetosphere and upper atmosphere. The resulting particle precipitation has been studied by polar orbiting satellites (*e.g.* HEIKKILA and WINNINGHAM, 1971; CRAVEN and FRANK, 1978; MENG, 1983). In this study we use particle data from satellite HILAT, launched on June 27, 1983 into a near circular, 800-km high orbit with an 82° inclination (POTOCKI, 1984).

The dayside auroral emissions are one result of the penetration into the magnetosphere and subsequent precipitation of magnetosheath plasma. Combined with continuous observations from the solar wind these emissions can be used as a diagnostic tool in the study of solar wind-magnetosphere interaction.

Only ground observations allow continuous monitoring of the auroral emissions. Due to the inaccessibility of the polar regions which satisfy the observation conditions, *i.e.* correct distance to the geomagnetic pole and so far north in geographic latitude that the sunlight does not disturb the observations at magnetic midday, the cusp aurora has received markedly less attention than the night-time aurora.

This article is based on optical observations from the ground on Svalbard, an island group to the north of Norway, east of Greenland. Section 2 contains coordinated satellite and ground observations of particle precipitation and optical emissions in the polar cusp. Ionospheric conductivities resulting from the particle precipitation are calculated. In Section 3 cases are presented showing cusp auroral dynamics in response to changes in the solar wind. Attention is focused on large-scale behaviour of the midday sector of the oval as well as more small-scale dynamics of individual auroral forms in the midday cusp. The different events presented in Sections 2 and 3 are discussed in Section 4. The emphasis is placed on solar wind-magnetosphere coupling mechanisms, by combining the available information from different levels of the coupling process.

2. Optical and Particle Characteristics of the Polar Cusp

Figure 1 shows one passage of satellite HILAT between Greenland and Svalbard on December 24, 1983. Also shown is the scanning direction of a four-channel meridian scanning photometer placed at Longyearbyen (LYR), Svalbard (geographic coordinates: 78.2°N , 15.7°E ; geomagnetic coordinates: 74.4° , 130.9°). By this technique the midday aurora can be observed within the range $69\text{--}80^{\circ}$ geomagnetic latitude. Local magnetic noon at the optical recording site corresponds to ~ 0830 UT. This means that the satellite pass shown in Fig. 1 occurred just prenoon. Photometer observations made during the time of the satellite pass are shown in Fig. 2. Each scan takes 12 s. To the left in Fig. 2a is shown the signature of a stable red (OI 630.0

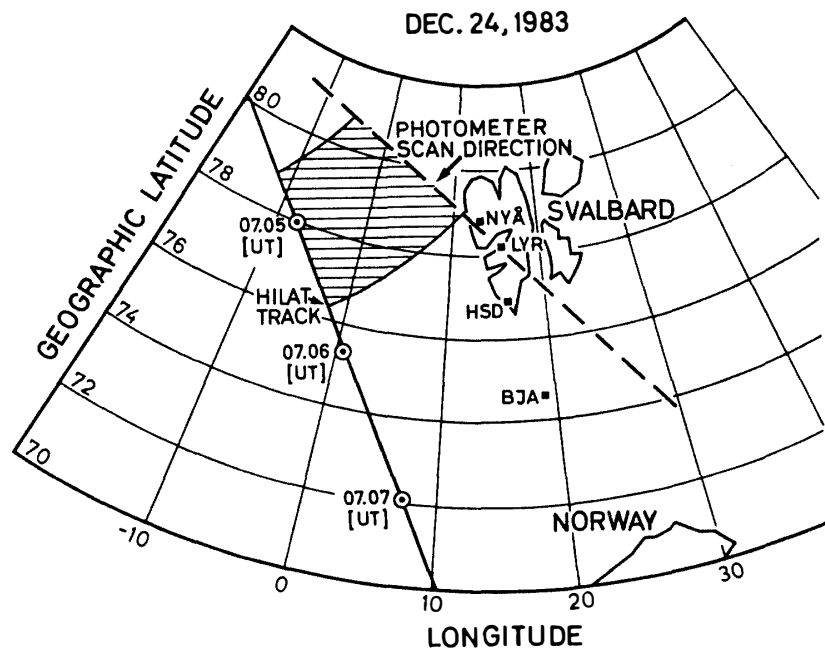


Fig. 1. Map showing the recording sites at Longyearbyen (LYR), Ny-Ålesund (NYÅ) and Hornsund (HSD), Svalbard, with the photometer scanning direction (dashed line) as well as the track of satellite HILAT, measuring electron precipitation above the ionosphere. The hatched area shows the projection of the polar cusp, as indicated by optical emissions and electron precipitation (cf. Fig. 3).

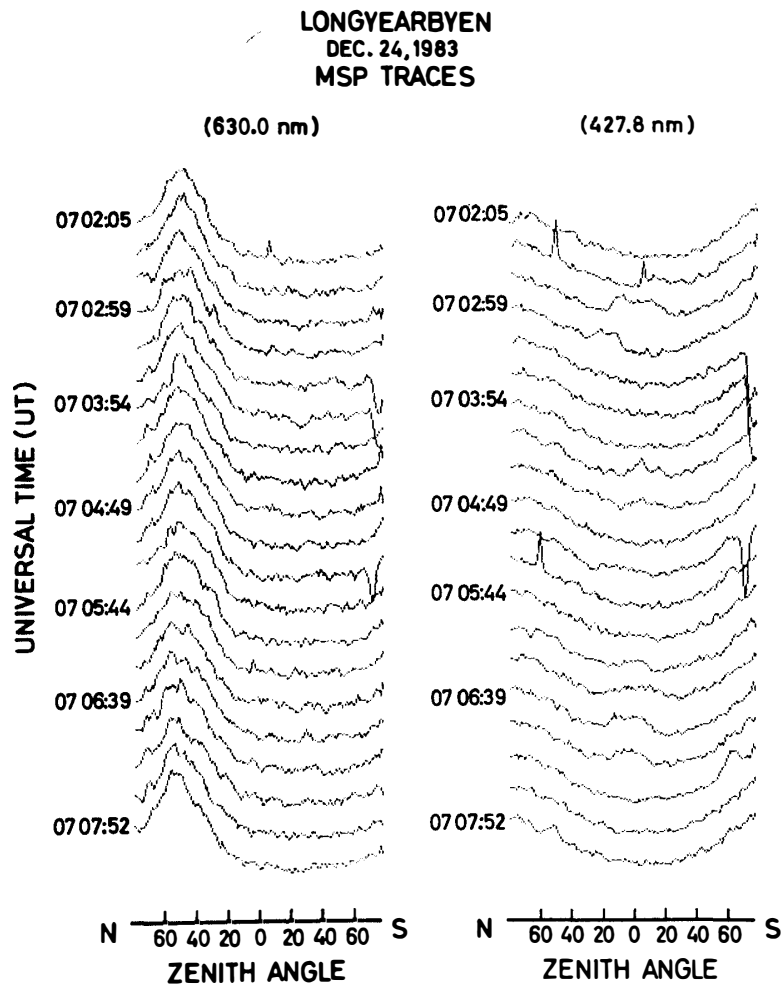


Fig. 2a. Meridian scanning photometer (MSP) recordings of polar cusp auroral emissions at 630.0 and 427.8 nm. Absolute intensities are given in Fig. 2b lower case b.

nm) belt of luminosity to the north of Longyearbyen. The observed intensity of a few kilorayleighs is typical for the red oxygen line in the quiet midday cusp (*cf.* DEEHR *et al.*, 1980). The corresponding recording of the blue band at 427.8 nm, from N_2^+ , shows a few enhancements near zenith ($\sim 150R$), above the background profile due to the Van Rijn effect. In the upper panel of Fig. 3 is plotted the intensity of the red line *versus* geomagnetic latitude, using 300 km (assumption) as the emission altitude. To the north of $30^\circ N$ (zenith angle) the green oxygen line at 557.7 nm did show a similar elevation profile as the red line with a maximum of ~ 500 rayleighs above the background (*cf.* Fig. 2b). At ~ 0706 UT the green line, like the blue band, shows an enhancement between $30^\circ N$ and $10^\circ S$ (zenith angle), with max intensity ~ 1 kR (557.7 nm), corresponding to the plasmasheet-like electron spectra observed to the south of the cusp (*cf.* Figs. 2b, 3, 4).

The lower section of Fig. 3 shows electron data obtained from HILAT during the pass shown in Fig. 1. Each electron analyzer consists of three basic components: an aperture system, a set of two concentric cylindrical curved plates, and a set of channeltrons. The detectors measure electrons in 16 channels between 20 and 20000

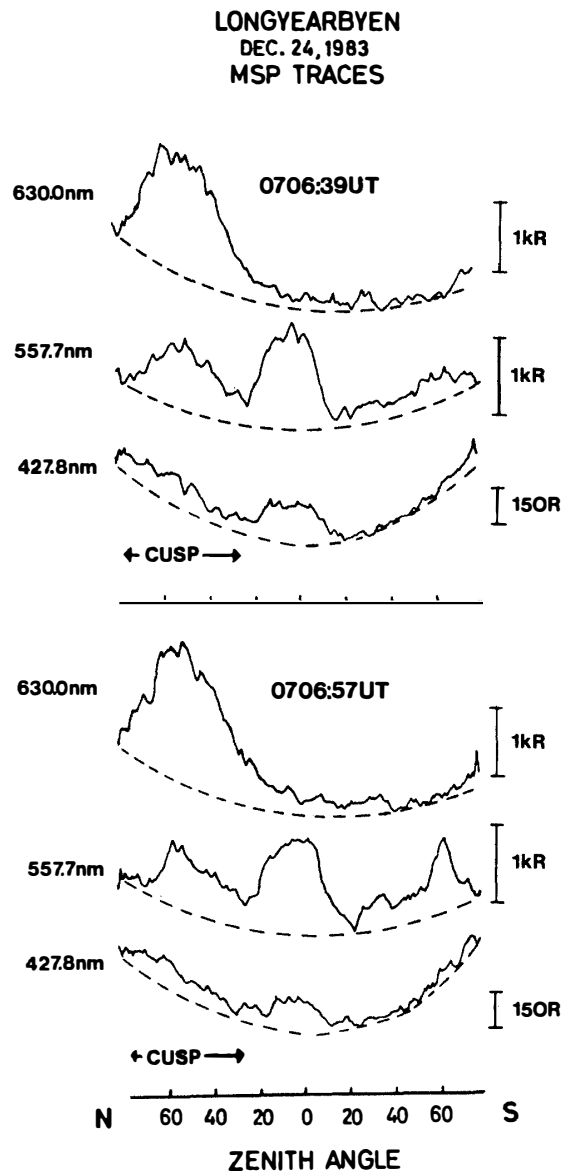


Fig. 2b. MSP traces of red and green oxygen lines as well as the N_2^+ blue band at 427.8 nm. Notice a typical cusp signature in the north. The luminosity around zenith shows a different spectral composition. The weak red line there is due to quenching below ~ 150 km.

eV (cf. HARDY *et al.*, 1984). The technique provides four 16-point spectra over this energy range each second in three different directions, corresponding to a spatial resolution of 1.8 km. The data in Fig. 3 are 1 s averages of recordings from the zenith detector. Latitude profiles of the average energy, the energy flux and the number flux are shown. Due to different particle characteristics we have defined three different latitude regions. The region between the two vertical lines is identified as the "particle cusp". Typical parameters for the electron precipitation in this region are 0.1 keV (average energy), 10^8 keV/(cm² sr s) (energy flux) and 10^8 (cm² sr s)⁻¹ (number flux). The above value for the differential energy flux corresponds to an integrated flux of $5 \cdot 10^{-4}$ W/m² (or 0.5 erg/(cm² s)). The cusp precipitation shows a sharp boundary towards the south, collocated with the equatorward boundary of the red

Dec. 24, 1983

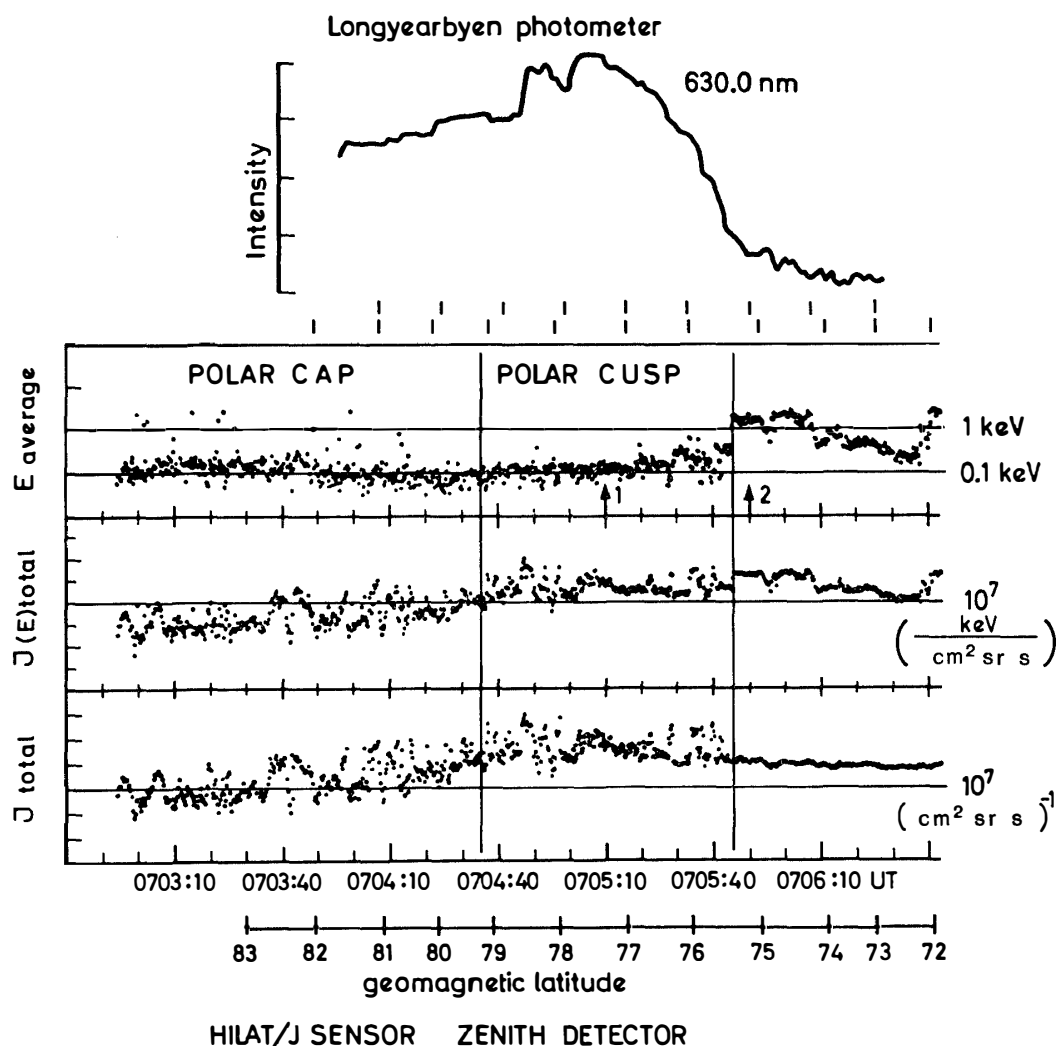


Fig. 3. Upper panel: Intensity of the red oxygen line at 630.0 nm versus geomagnetic latitude. The latitude profile is obtained by transforming from the elevation profiles in Fig. 2, using an estimated emission altitude of 300 km.

Lower panel: Electron data obtained from satellite HILAT showing average energy, differential energy flux and differential number flux in logarithmic scale versus geomagnetic latitude and time (UT). Vertical lines mark boundaries between regions showing different particle characteristics, defined by the authors (see text). The satellite track is shown in Fig. 1.

belt of luminosity. The average particle energy and the number flux on the equatorward side of the boundary are ~ 1.5 keV and 10^3 $(\text{cm}^2 \text{ sr s})^{-1}$, respectively. We also notice that the southern boundary of the cusp defines a sharp boundary in terms of scatter in the data points. The particle precipitation in the cusp and the polar cap is characterized by much more structure (irregularities) than further south. The northern boundary of the "particle cusp" is not that sharp as the southern boundary.

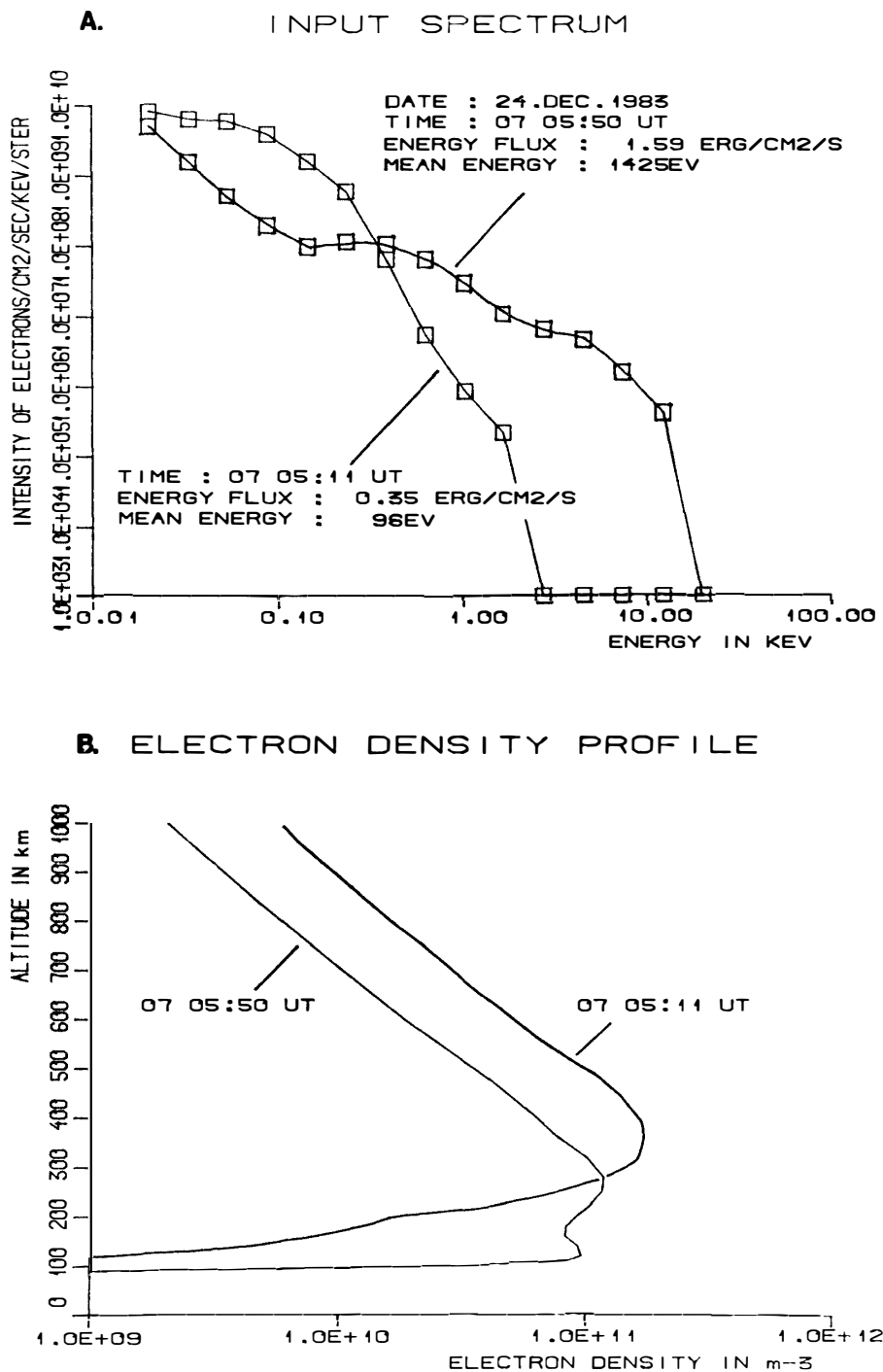
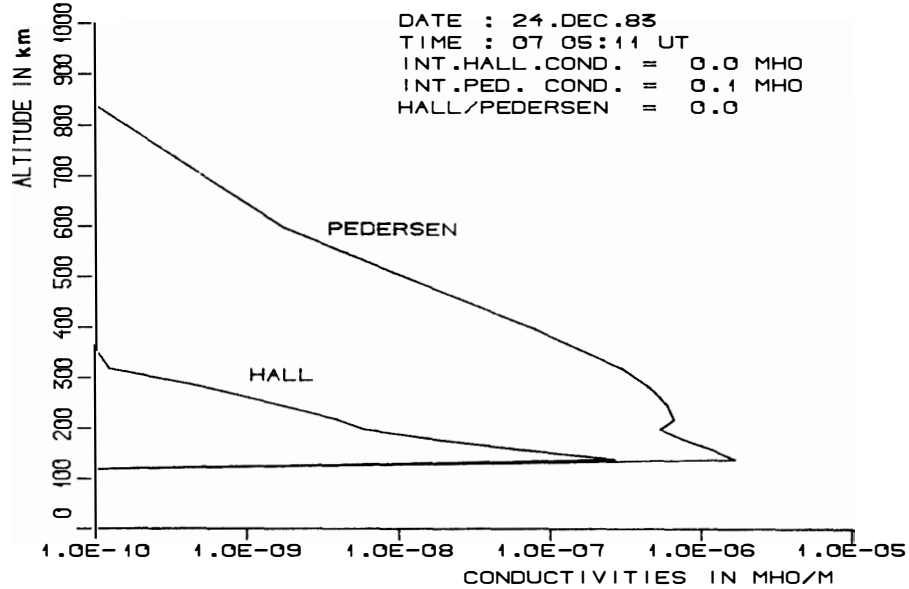


Fig. 4. A: Electron input spectra at 0705:11 and 0705:50 UT, corresponding to arrows 1 and 2 in Fig. 3.

B: Ionospheric density profiles calculated from particle input spectra shown in Fig. 4A.

However, a gradual decrease in the number flux and the energy flux do occur towards higher latitudes. Typical values for the electron parameters in the polar cap in this case are 0.2 keV (average energy), 10^6 keV/(cm² sr s) (energy flux) and $5 \cdot 10^6$ (cm² sr s)⁻¹ (number flux). Thus, the electron energy flux is a factor 100 less intense in the polar cap as compared to the polar cusp.

C. CONDUCTIVITY PROFILES



CONDUCTIVITY PROFILES

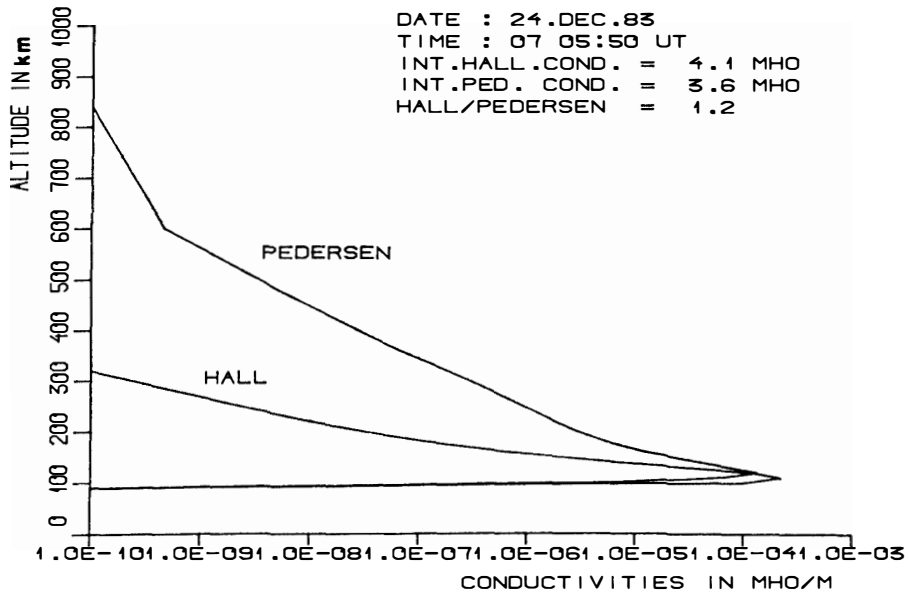


Fig. 4. C: Altitude profiles of Pedersen and Hall conductivities calculated from the same particle spectra as shown in Fig. 4A. Height-integrated conductivities are listed.

Figure 4 shows energy spectra of precipitating particles at 0705:11 and 0705:50 UT as well as the resulting electron density and conductivity profiles. The 0705:11 UT spectrum is typical for the cusp region (arrow 1 in Fig. 3), with an energy flux of 0.35 erg/(cm² s) and a mean energy of 96 eV. The corresponding electron density profile shows a maximum of $\sim 2 \cdot 10^{11} \text{ m}^{-3}$ at ~ 370 km. The other spectrum (0705:

50 UT), which was measured to the south of the cusp (arrow 2 in Fig. 3) is characterized by an energy flux of $1.6 \text{ erg}/(\text{cm}^2 \text{ s})$ and a mean energy of 1.4 keV. The resulting density profile shows distinct *E*- and *F*-layers with peak values of $\sim 10^{11} \text{ m}^{-3}$ at ~ 120 and 280 km, respectively.

Altitude profiles of Hall and Pedersen conductivities are shown in section C of Fig. 4. Values of the height-integrated Hall and Pedersen conductivities produced by particle precipitation are 0.0 and 0.1 mhos for the central cusp region and 4.1 and 3.6 mhos to the south of the cusp.

We notice an enhanced level of the electron mean energy in the southern part of the cusp region (*cf.* Fig. 3). The integrated energy flux at 0705:30 UT (midway between arrows 1 and 2) is $0.2 \text{ erg}/(\text{cm}^2 \text{ s})$, with a mean energy of 220 eV. The corresponding Hall and Pedersen conductivities are 0.6 and 0.9 mhos. In the central polar cap we would expect a typical value for the Pedersen conductivity to be ~ 0.5 mhos. (Complete electron spectra not available for this study.)

The calculations of ionospheric density and conductivity profiles are based on models and data from the following publications: REES (1963, 1969), JONES and REES (1973), U. S. STANDARD ATMOSPHERE (1976), WALLIS and BUDZINSKI (1981) (electron collision frequency), VICKREY *et al.* (1981) (ion collision frequency), MARKLUND *et al.* (1981) (effective recombination coefficient).

3. Auroral Dynamics in the Polar Cusp

3.1. Large-scale auroral dynamics in the midday sector

Figure 5 shows the latitudinal location of the polar cusp aurora (OI 630.0 nm) in relation to disturbances in the local magnetic field and in the nightside field (Alaska). Between 0820 and 1000 UT the auroral belt of luminosity moved equatorward by about 5° geomagnetic latitude. Superposed on this general trend are a few northward excursions of luminosity. Between 10 and 11 UT the auroral light moved back to the initial location with the center about 50° (zenith angle) to the north of Longyearbyen (LYR). The local magnetic field was recorded at Ny-Ålesund (NYÅ), 117 km to the north of Longyearbyen (*cf.* Fig. 1). Data from satellite IMP-J for January 16, 1984 show that the IMF vector was rather stable between 09 and 10 UT, with the following component values (SE coordinates): $B_x \simeq B_z \simeq -3.5 \text{ nT}$, $B_y \simeq 0$ ($B_{\text{total}} = 5 \text{ nT}$). Unfortunately, there were gaps in the recordings both before and after this interval. The location of the satellite at 09 UT was given by the following coordinates in the earth-centered solar ecliptic system: $5.4 R_E(\text{X})$, $35.3 R_E(\text{Y})$, $17.7 R_E(\text{Z})$. The radial distance was $39.9 R_E$.

We do observe a clear correlation between southward expansions of the aurora and negative deflections in the *H*-component of the local magnetic field. Maximum deflection from the quiet-time level at Ny-Ålesund was 100 nT. On the nightside (College, Alaska) a substorm intensification was recorded between 0905 and 0910 UT. Maximum deflection at ~ 0940 UT was -800 nT . Inspection of magnetograms from the Alaska chain of stations shows that College (65° geomagnetic latitude) was near the center of the electrojet at that time.

The contour-plot in the middle panel of Fig. 6 is a three-dimensional representa-

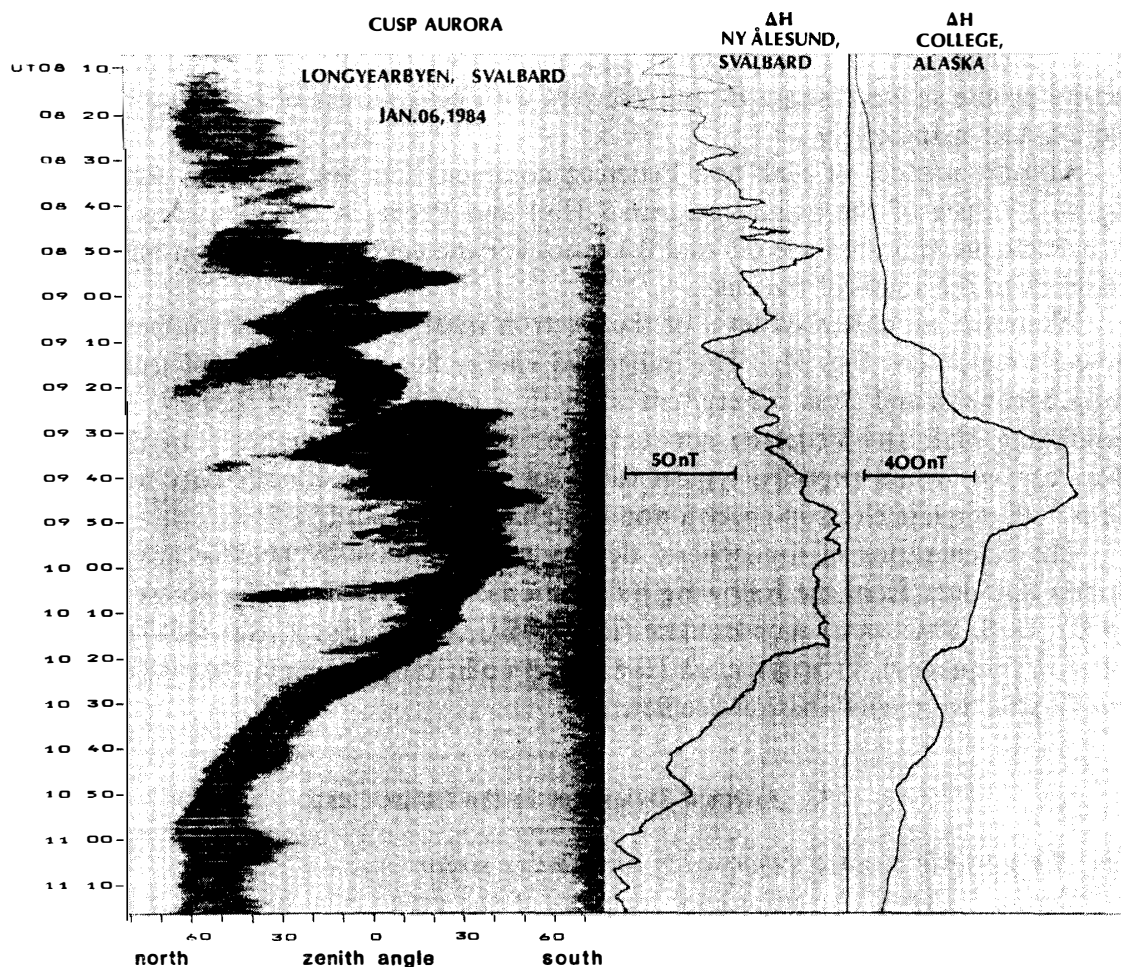


Fig. 5. *Left:* Location in zenith angle of the polar cusp aurora (OI 630.0 nm) as a function of universal time (12 MLT=0830 UT). The plot is obtained from MSP recordings as shown in Fig. 2.

Middle: The horizontal component of the local magnetic field at Ny-Ålesund (NYÅ) (see Fig. 1). Negative deflection is towards the right.

Right: The horizontal component of the magnetic field at College, Alaska, close to the magnetic midnight meridian (24 MLT=11 UT).

tion of the red oxygen emission (630.0 nm) above Svalbard on January 16, 1981. From ~0710 UT we observe a significant thinning and equatorward shift of the oval. This is identified as the response to a significant transition of the magnetosheath magnetic field from northward to southward orientation occurring slightly before 07 UT (see ISEE-1 data in upper frame). A sharp transition back to northward field orientation was recorded at ~0750 UT. This was followed by a northward contraction of the auroral belt near 08 UT. The location of the aurora was mainly unchanged between 0830 and 1010 UT. Then it again shifted southward. This was preceded by a distinct southward change of the magnetic field at ~0955 UT. At 1020 UT B_z was almost back to zero, before another southward transition took place. The oval location was unchanged between 1015 and 1035 UT, then it moved steadily southward again. This southward expansion was associated with brightening and

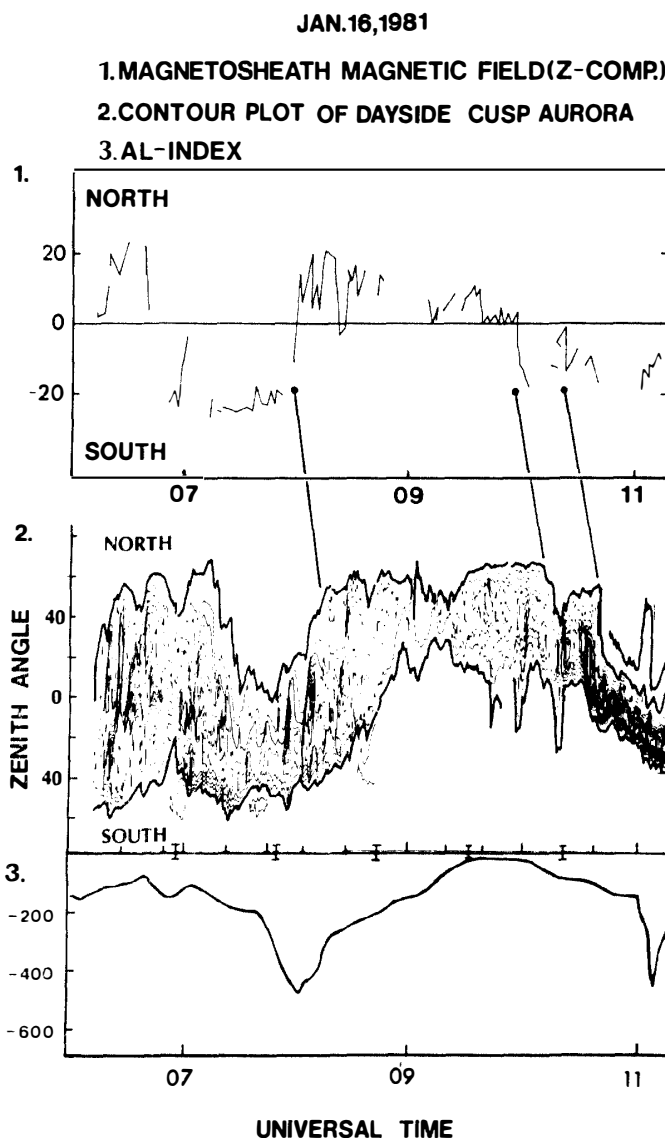


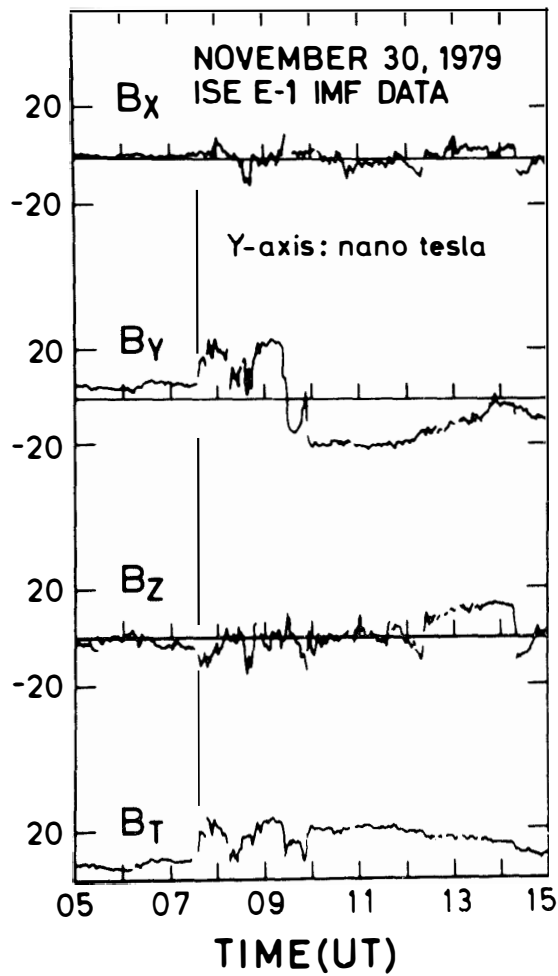
Fig. 6. 1: Magnetic field Z-component measured from spacecraft ISEE-1 within the magnetosheath (amplified by a factor 3 relative to the corresponding IMF component). The vertical scale is in nanoteslas.
2: Contour plot of dayside aurora (630.0 nm) observed at Longyearbyen, Svalbard, on January 16, 1981. Intensity levels are in steps of 1 kR starting at 3 kR.
3: AL-index in nanoteslas. (After SANDHOLT *et al.*, 1985).

thinning of the oval aurora.

The lower panel of Fig. 6 shows the *AL*-index. At the times of substorm onset we do not observe any distinct response in the dayside aurora. Southward transitions of the exterior *B*-field are followed by ~ 1 hour periods with increasing negative deflection (~ 100 nT) in the *AL*-index, before substorm onsets.

3.2. Small-scale cusp auroral dynamics

In this section a different event is presented, showing more small-scale dynamical behaviour of the cusp aurora and the local magnetic field following a discontinuity



GEOMAGNETIC DATA
NOV. 30, 1979

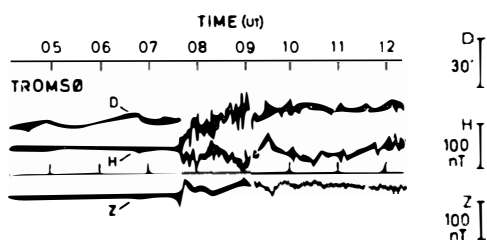
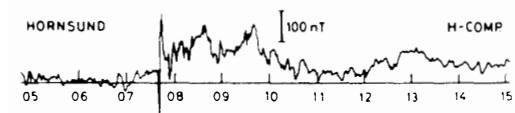
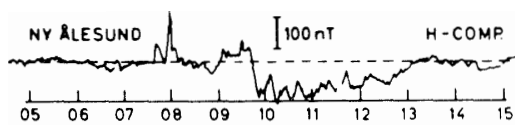


Fig. 7. Upper: ISEE-1 magnetic field data from outside the bowshock.

Lower: Geomagnetic data from ground stations on Svalbard (Ny-Ålesund, Hornsund) and from Tromsø (Northern Norway) (see Fig. 1). (After SANDHOLT *et al.*, 1985).

in the solar wind impinging on the frontside magnetosphere.

A factor 3 increase of the interplanetary magnetic field was detected by satellite ISEE-3 ($240 R_E$ upstream) at ~ 0645 UT on November 30, 1979. The corresponding amplification reached ISEE-1, just outside the bowshock, at ~ 0735 UT (*cf.* Fig. 7). This IMF compression was followed by a geomagnetic sudden commencement (SC) at 0739 UT. Figure 7 shows the signatures of the SC at the ground stations Ny-Ålesund, Hornsund and Tromsø (geomagnetic latitudes: 75.4; 73.5; 67.1, *cf.* Fig. 1).

A phenomenon to notice in Fig. 7 is the general modulation of the magnetic field of the cusp region by the IMF B_y -component.

The relative amplitude of disturbance in the H -component at the two stations Ny-Ålesund and Hornsund changes as the aurora moves in latitude between these stations. Between 08 and 10 UT the largest response ($\Delta H/IMF-B_y$) is seen at Hornsund, when the center of the aurora is close to that latitude. Between 10 and 12 UT the belt of luminosity extends to higher latitudes. This change in auroral extension is accompanied by an increase in the ratio $\Delta H/IMF-B_y$ at Ny-Ålesund. A typical value of this ratio when the aurora is nearly overhead is 5.

The first signature in the cusp aurora following the sudden commencement was an enhancement of the auroral emissions at 427.8, 557.7 and 630.0 nm at 0740 UT (not shown in Fig. 8). The maximum intensity at 630.0 nm increased from below 1 kR to ~ 5 kR. During the next 15 min, from 0741 to 0756 UT, the aurora was very stable in intensity, form and location.

The main intensification during the whole midday period occurred at 0757 UT, when a bright red corona of visible intensity was switched on (*cf.* Fig. 8). During the following 5 min (0757–0802 UT) the bright form moved poleward with an average drift speed of ~ 750 m/s. A maximum intensity of 40 kR in the red line was reached at 0802 UT while the green line (not shown) was generally decreasing in intensity after the initial intensification at 0757 UT, with a maximum of 2 kR. This trend was interrupted by two minor transient enhancements at 0759 and 0802 UT. Similar intensifications and associated poleward expansions as that between 0757 and 0802 UT, although not that bright, were observed during the following intervals: 0812–0817 UT, 0820–0824 UT, 0859–0904 UT, 0910–0916 UT, 0921–0926 UT, 0928–0934 UT. Notice that five minutes is a typical time for each luminosity burst.

Figure 8 illustrates the connection between dynamical behaviour of the cusp aurora and local magnetic pulsations during this event. The upper panel shows intensity contours of the 630.0 nm emission in elevation-time coordinates obtained from the meridian scanning photometer (MSP). We recall the strong intensification and the associated latitudinal expansion starting at 0757 UT. Two other brightenings/expansions, in the intervals 0812–0817 and 0820–0824 UT, are also shown. In the lower panel are plotted the recorded pulsations in the Y -component of the local magnetic field (the X -component is missing). The pulsation activity during this period started with a transient impulse at the time of the SC (0739 UT). From 0740 UT the average level of pulsation activity was well above the pre-existing activity for several hours.

A close correlation between the auroral intensity and the amplitude of the local Pi-type pulsations is recognized. These short periodic pulsations are superposed on

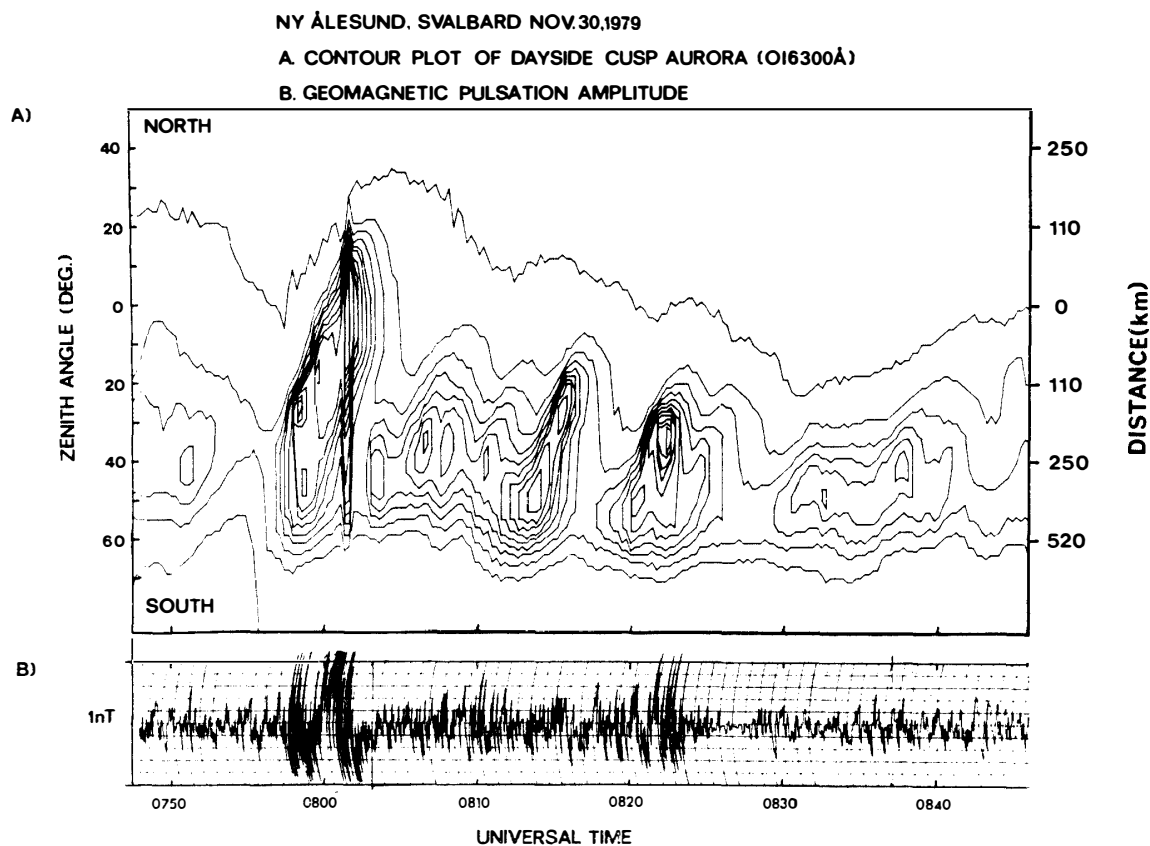


Fig. 8. A: Midday cusp auroral luminosity (red oxygen line) in zenith angle versus time coordinates obtained from meridian photometer scans as shown in Fig. 2. Intensity levels are in steps of 2 kR starting at 1 kR. Distance from zenith in north-south direction is given to the right, assuming an emission altitude of 300 km. B: Magnetic Y-component pulsation amplitude. Full scale is 1 nanotesla. (After SANDHOLT *et al.*, 1985).

more slow variations. Pronounced events of associated auroral brightening/latitudinal expansions and geomagnetic pulsation activity were also observed during the time intervals 0910–0916 and 0928–0934 UT (not shown). They were local events associated with bursts of auroral luminosity (particle precipitation) in the cusp.

4. Discussion

4.1. The December 24, 1983 event

One main purpose of a coordinated study of particle- and optical observations from the polar cusp is to investigate the interaction between the soft flux of precipitating electrons and the upper atmosphere, including ionization and excitation mechanisms. By making simultaneous measurements of the particle input from the satellite and the optical output from the ground we are in a position to test existing models of the energy transfer mechanisms. One interesting question is the contribution to the red line intensity from thermal excitation (*cf.* WICKWAR and KOFMAN, 1984).

There are, however, some practical problems associated with this kind of study.

The following observation conditions are required: a stable auroral form close to magnetic zenith when the satellite is passing above the observing site at midday. These requirements are not to be satisfied very often.

The HILAT satellite has an orbit period of 102 min with a solar precession rate of -7.5 min per day. Thus, the earth rotates approximately 25 degrees per satellite orbit. On December 24, 1983 the preceding pass (~ 0525 UT) relative to that shown in Fig. 1 occurred close to the observing site at Longyearbyen (LYR). However, since that pass occurred 3 hours prenoon (magnetic local time) it was not a typical cusp pass. Thus, the 0705 UT pass was the best one this day, even though it was not close to the ground site. In order to relate the satellite and ground data in this case we have to be sure that there was a strong east-west homogeneity within the shaded region in Fig. 1.

The requirement of a quiet form close to the zenith above Svalbard does not occur frequently. A quiet auroral condition happens when the magnetosphere is in a quiet state, which is associated with a contracted auroral oval. The midday cusp is then located to the north of our recording site as illustrated in Fig. 2. Thus, the December 24, 1983 case is not specially relevant for our main purpose, *i.e.* the study of upper atmosphere excitation processes due to low-energy electron precipitation. Until better events are found we have used the HILAT electron data to calculate electron density and conductivity profiles for the cusp ionosphere, as described in Section 2. As we will see, these parameters are highly relevant for the discussion of small-scale cusp dynamics.

4.2. The January 16, 1981 and January 6, 1984 events

Southward and northward transitions of the magnetosheath magnetic field on January 16, 1981 were followed within 15 min by equatorward and poleward shifts of the auroral belt in the midday sector (Fig. 6). Because of missing data in the IMP-J IMF recordings on January 6, 1984 we don't know if the observed equatorward and subsequent poleward movements shown in Fig. 5 are related to changing IMF orientation. Figures 5 and 6 show equatorward expansions of the midday aurora to be closely associated with DP2-type magnetic disturbances. The onset of geomagnetic substorms was not observed to have any clear effect on the midday aurora.

From these data and those presented in SANDHOLT *et al.* (1983) we conclude that IMF B_z is a major influence on the large-scale dynamic motion of the midday aurora (*cf.* also MENG, 1983). We note that the ISEE-3 IMF data should be used with caution in this type of study, because the precise timing of the arrival at the Earth of the observed IMF structure is a serious problem. The time delay between the ISEE-3 location and the earth is shown to be highly variable (RUSSELL *et al.*, 1980; CROOKER *et al.*, 1982).

Several events showing no relationship between substorm activity and dayside auroral dynamics are observed (SANDHOLT *et al.*, 1983). Thus, not all substorms have an effect on the dayside aurora. This does not mean that IMF B_z necessarily is the only influence. Cases showing a close relationship between substorms and latitudinal movements of the dayside aurora are reported by EATHER *et al.* (1979). According to one model auroral oval expansions and contractions are considered to

be the net result of dayside merging and nightside reconnection (*cf.* AKASOFU, 1977, p. 210).

Our observations seem to be in favour of the view that the energy supply from the solar wind gives rise to different modes of energy dissipation in the magnetosphere and upper atmosphere; one directly driven by solar wind-magnetosphere dynamo mechanisms and another more explosive release of energy stored in the magnetotail (unloading process), constituting the expansion phase of the substorm (*cf.* NISHIDA, 1983). Manifestations of the driven process are coherent modulations of region 1 field-aligned current (IJIMA and POTEIRA, 1982; SANDHOLT and ÅSHEIM, 1985), the DP2 component of the geomagnetic disturbance field and expansion/contraction of the auroral oval (*cf.* Fig. 6, periods 0630–0730 and 1000–1100 UT).

4.3. *The November 30, 1979 event*

An amplification of the interplanetary magnetic field by a factor 3 was followed by Pi-type magnetic pulsations and enhanced auroral luminosity in the midday cusp region. These enhanced levels of activity persisted for some hours. Short-lived (~ 5 min) bursts of auroral brightening/latitudinal expansions were accompanied by local intensifications of the Pi-activity. Magnetograms from local ground stations in the cusp region show a clear DPY component of the geomagnetic disturbance field, which is often reported in the summer hemisphere (*cf.* TROSHICHEV, 1982).

The observed optical spectral ratio (1630.0 nm/1557.7 nm) during the events of luminosity burst and enhanced Pi-activity—ranging between 10 and 40—indicates relatively soft particle spectra. Thus, the main part of the particle flux does not affect the state of *E*-layer ionization. However, the increase of the ratio $\Delta H/IMF-B_y$ when the aurora comes close to the observing station (Figs. 7, 8) indicates that the high-energy tail of the particle spectrum has some effect on the *E*-layer conductivity (*cf.* PRIMDAHL and SPANGSLEV, 1981). Notice the positive spike in the Ny-Ålesund magnetogram at ~ 0800 UT when the bright red aurora expanded up to the station. Increased response in the local magnetic disturbance at Ny-Ålesund was observed from ~ 10 UT onwards (Fig. 7), when the luminosity covered a larger latitudinal extension (not shown), including both Ny-Ålesund and Hornsund latitudes.

In the following we will discuss the more small-scale auroral intensifications in the cusp region (Fig. 8) in relation to the phenomenon of impulsive penetration of magnetosheath plasma irregularities into the magnetosphere, reported most recently by LUNDIN (1984) (*cf.* also LEMAIRE *et al.*, 1979). Particle observations in the low-altitude cusp region (satellite- and rocket-data) consistent with the idea of impulsive entry from the magnetosheath are reported by MAYNARD and JOHNSTONE (1974) and TORBERT and CARLSON (1976).

LUNDIN proposed an MHD model for the observed plasma penetration, generating a local *E*-field in the magnetospheric boundary layer, powering an electric current system transferring energy to the ionosphere. An estimate of the range of lifetimes for a penetrating plasma element, representing the order of magnitude of the decay time of the energy transfer process, as observed in the dayside high-latitude ionosphere, was given. According to this model the time of duration of the dissipation event is regulated by the Pedersen conductivity of the polar cusp ionosphere.

Typical values were inferred to be a few minutes, corresponding to an ionospheric conductivity of the order of 1 mho. Lifetimes like these compare well with the duration of the observed optical intensification and the associated magnetic pulsation enhancement in the cusp region. The value used for the Pedersen conductivity (1 mho) is consistent with those values calculated in Section 2 for the December 24, 1983 case. In that case we found Σ_p values between 0.1 and 0.9 mhos within the quiet cusp, corresponding to mean energies of the precipitating electrons between 100 and 200 eV. The corresponding Hall conductivities were between 0.0 and 0.6 mhos. The upper limits of these ranges are considered to be reasonable values for the cusp auroral burst at 08 UT on November 30, 1979. A relatively weak E -layer ionization ($\Sigma_H \sim 0.5$ mhos) may give rise to the observed enhanced amplitude of deflection in the local magnetic field (*cf.* Figs. 7 and 8).

Phenomena with some similarity to the impulsive plasma penetrations mentioned above are the so-called flux transfer events reported by RUSSELL and ELPHIC (1979) (*cf.* also RIJNBEEK *et al.*, 1984). As the impulsive injection model was first suggested for interactions of the solar wind with a closed magnetosphere, the flux transfer events, which are most frequently observed when IMF- B_z is negative, are explained in term of a transient reconnection process. HEIKKILA (1982) has discussed impulsive injections in relation to an open magnetic field geometry, indicating that the magnetopause reconnection (flux transfer events) and impulsive plasma injections are phenomena which may coexist and interact (BURCH, 1983).

The main optical event on November 30, 1979 (~ 08 UT) occurred at the time of negative IMF B_z . The optical spectral characteristics, the time of duration, the drift motion and the repetition frequency of cusp intensifications like this are consistent with the expected optical signatures of flux transfer events (S.W.H. COWLEY, private communication, 1985).

Acknowledgements

We express our thanks to Drs. V. A. TROITSKAYA (Institute of Physics of the Earth, Moscow, USSR) and C. T. RUSSELL (University of California, Los Angeles, USA) for providing magnetometer data from ground station Ny-Ålesund (pulsation data) and spacecraft ISEE-1, respectively. IMP-J data were provided by Dr. T. L. AGGSON (Goddard Space Flight Center, Maryland, USA). We also acknowledge the magnetic information we have received from College, Alaska (Geophysical Institute, Fairbanks, Alaska), Svalbard stations Ny-Ålesund (University of Tromsø) and Hornsund (Polish Geophysical Institute) and World Data Center, Copenhagen, Denmark.

References

- AKASOFU, S.-I. (1977): *Physics of Magnetospheric Substorms*. Dordrecht, D. Reidel, 280 p. (Astrophys. Space Sci. Lib., Vol. 11).
- BURCH, J. L. (1983): *Energy transfer in the quiet and disturbed magnetosphere*. U. S. National Report to International Union of Geodesy and Geophysics 1979-1982, Washington, D. C., Am. Geophys. Union, 463.
- CRAVEN, J. D. and FRANK, L. A. (1978): *Energization of polar cusp electrons at the noon meridian*. *J. Geophys. Res.*, **83**, 2127-2132.

- CROOKER, N. U., SISCOE, G. L., RUSSELL, C. T. and SMITH, E. J. (1982): Factors controlling degree of correlation between ISEE 1 and ISEE 3 interplanetary magnetic field measurements. *J. Geophys. Res.*, **87**, 2224–2230.
- DEEHR, C. S., SIVJEE, G. G., EGELAND, A., HENRIKSEN, K., SANDHOLT, P. E., SMITH, R., SWEENEY, P., DUNCAN, C. and GILMER, J. (1980): Ground-based observations of *F*-region aurora associated with the magnetospheric cusp. *J. Geophys. Res.*, **85**, 2185–2192.
- EATHER, R. H., MENDE, S. B. and WEBER, E. J. (1979): Dayside aurora and substorm current systems. *J. Geophys. Res.*, **84**, 3339–3359.
- HARDY, D. A., HUBER, A. and PANTAZIS, J. A. (1984): The electron flux J censor for HILAT. Johns Hopkins APL Technical Digest. April–June 1984.
- HEIKKILA, W. J. (1982): Impulsive plasma transport through the magnetopause. *Geophys. Res. Lett.*, **9**, 159–162.
- HEIKKILA, W. J. and WINNINGHAM, J. D. (1971): Penetration of magnetosheath plasma to low altitude through the dayside magnetospheric cusp. *J. Geophys. Res.*, **76**, 883–891.
- IJIMA, T. and POTEMRA, T. A. (1982): The relationship between interplanetary quantities and Birke-land current densities. *Geophys. Res. Lett.*, **9**, 442–445.
- JONES, R. A. and REES, M. H. (1973): Time dependent studies of the aurora-I. Ion density and composition. *Planet. Space Sci.*, **21**, 537–557.
- LEMAIRE, J., RYCROFT, M. J. and ROTH, M. (1979): Control of impulsive penetration of solar wind irregularities into the magnetosphere by the interplanetary magnetic field orientation. *Planet. Space Sci.*, **27**, 47–57.
- LUNDIN, R. (1984): Solar wind energy transfer regions inside the dayside magnetopause—II. Evidence for an MHD generator process. *Planet. Space Sci.*, **32**, 757–770.
- MAYNARD, N. C. and JOHNSTONE, A. D. (1974): High-latitude dayside electric field and particle measurements. *J. Geophys. Res.*, **79**, 3111–3123.
- MARKLUND, G., SANDAHL, I. and OPGENOORTH, H. (1981): A study of the dynamics of a discrete auroral arc. *Electron and Plasma Physics*. Royal Institute of Technology, S-10044 Stockholm, Sweden.
- MENG, C. I. (1983): Case studies of the storm time variations of the polar cusp. *J. Geophys. Res.*, **88**, 137–149.
- NISHIDA, A. (1983): IMF control of the earth's magnetosphere. *Space Sci. Rev.*, **34**, 185–200.
- POTOCKI, K. A. (1984): The HILAT spacecraft. Johns Hopkins APL Technical Digest. April–June 1984.
- PRIMDAHL, F. and SPANGSLEV, F. (1981): Cusp region and auroral zone field aligned currents. *Ann. Geophys.*, **37**, 529–538.
- REES, M. H. (1963): Auroral ionization and excitation by incident energetic electrons. *Planet. Space Sci.*, **11**, 1209–1218.
- REES, M. H. (1969): Auroral electrons. *Space Sci. Rev.*, **10**, 413–441.
- RIJNBEEK, R. P., COWLEY, S. W. H., SOUTHWOOD, D. J. and RUSSELL, C. T. (1984): A survey of dayside flux transfer events observed by ISEE 1 and 2 magnetometers. *J. Geophys. Res.*, **89**, 786–800.
- RUSSELL, C. T. and ELPIC, R. C. (1979): ISEE observations of flux transfer events at the dayside magnetopause. *Geophys. Res. Lett.*, **6**, 33–36.
- RUSSELL, C. T., SISCOE, G. L. and SMITH, E. J. (1980): Comparison of ISEE 1 and 3 interplanetary magnetic field observations. *Geophys. Res. Lett.*, **7**, 381–384.
- SANDHOLT, P. E. and ÅSHEIM, S. (1985): The relationship between reconnection electric field, field-aligned and ionospheric currents. *Ann. Geophys.*, **3**, 43–50.
- SANDHOLT, P. E., EGELAND, A., LYBEKK, B., DEEHR, C. S., SIVJEE, G. G. and ROMICK, G. J. (1983): Effects of interplanetary magnetic field and magnetospheric substorm variations on the dayside aurora. *Planet. Space Sci.*, **31**, 1345–1362.
- SANDHOLT, P. E., EGELAND, A., HOLTET, J. A., LYBEKK, B., SVENES, K. and ÅSHEIM, S. (1985): Large and small-scale dynamics of the polar cusp. *J. Geophys. Res.*, **90**, 4407–4414.
- TORBERT, R. B. and CARLSON, C. W. (1976): Impulsive ion injections into the polar cusp. *Magneto-*

- spheric Particles and Fields, ed. by B. M. McCORMAC. Dordrecht, D. Reidel, 47–53 (Astrophys. Space Sci., Vol. 58).
- TROSHICHEV, O. A. (1982): Polar magnetic disturbances and field-aligned currents. *Space Sci. Rev.*, **32**, 275–360.
- U. S. STANDARD ATMOSPHERE (1976): NOAA-NASA-U. S. Air Force, Washington, D. C., October 1976.
- VICKREY, J. F., VONDRAK, R. R. and MATTHEWS, S. J. (1981): The diurnal and latitudinal variations of auroral-zone ionospheric conductivity. *J. Geophys. Res.*, **86**, 65–75.
- WALLIS, D. D. and BUDZINSKI, E. E. (1981): Empirical models of height integrated conductivities. *J. Geophys. Res.*, **86**, 125–137.
- WICKWAR, V. B. and KOFMAN, W. (1984): Dayside red auroras at very high latitudes; The importance of thermal excitation. *Geophys. Res. Lett.*, **11**, 923–926.

(Received January 31, 1985; Revised manuscript received July 18, 1985)